



Thermodynamic modelling and temperature sensitivity analysis of banana (*Musa spp.*) waste pyrolysis

Joshua O. Ighalo¹ · Adewale George Adeniyi¹

© Springer Nature Switzerland AG 2019

Abstract

Pyrolysis has been established as a good technique of recovering energy from biomass. In this study, a thermodynamic model was developed on ASPEN Plus V8.8 to study the temperature sensitivity and yield of products from the pyrolysis of different banana wastes. The wastes considered were banana peels, pseudo-stem and leaves. The model was validated with experimental results for pseudo-stem pyrolysis. From comparison, the pseudo-stem was observed to give a slightly higher yield of gas compared to the other residues. Thermodynamic predictions of gas yield are similar for the different feedstock at low temperatures but varying at higher temperatures with the leaves producing less. Furthermore, the yield of oil from leaves is less and that of char is higher than for the other residues. The fluid phase products (bio-oil and syn-gas) were higher for pseudo-stem than for the other residues due to greater proportion of volatile matter from the proximate analysis. The suitability of banana pseudo-stem for bio-oil production via pyrolysis is established in comparison with the other residues studied. The leaves and peel are more suitable for low-temperature thermochemical processing for bio-char production.

Keywords Pyrolysis · Banana · ASPEN Plus · Thermodynamics · Temperature sensitivity

1 Introduction

The banana (*Musa spp.*) plant erroneously referred to as a 'tree' is a large single-fruit bearing herb widely cultivated in West Africa [1]. It is tall and sturdy with a cylindrical stem and can grow to a height of 0.8 m to about 7.5 m [2]. In the process of harvesting (lifecycle is about 10–12 months), the plant is cut so a new shoot can grow from the stub. A lot of wastes/residues are generated from the harvesting and consumption of banana fruits, and these include rotten fruit, peels, empty fruit bunch, leaves, pseudo-stem and rhizome [3]. These residues have been used for a variety of non-energy applications which includes the extraction of useful bio-products [4, 5], in polymer composites [6, 7], in textiles [8], for preparing adsorbents and ion-exchangers [9, 10] and a host of others [11, 12]. Banana wastes possess a huge energy potential as have

been revealed from proximate, elemental, chemical and thermogravimetric analyses [1, 3, 13–19]. This informs that it would be a very good feedstock for thermochemical processes.

Pyrolysis is a quite popular technique in the recovery of energy from waste biomass. It is the heating of up of material feed to elevated temperatures under inert conditions [20]. The products formed are bio-oil, synthesis gas and char [20]. Banana waste has been pyrolysed for hydrogen production [21] and char production [22]. There are also other studies where banana wastes such as pseudo-stem [23, 24], leaves [16, 17, 24] and peel have been pyrolysed. Fernandes et al. [17] pyrolysed banana leaves and pseudo-stem at 500 °C for 60 min in a slow pyrolysis batch reactor. Oil yield was 28.8% for pseudo-stem and 23.9% for leaves. Char yield was 58.4% for pseudo-stem and 66.8% for leaves. Sellin et al. [16] carried out fast pyrolysis of banana

✉ Joshua O. Ighalo, oshea.ighalo@yahoo.com | ¹Chemical Engineering Department, Faculty of Engineering and Technology, University of Ilorin, P. M. B. 1515, Ilorin, Nigeria.



leaves in a fluidised bed reactor. They obtained 49.6% gas, 27.0% bio-oil and 23.3% char. Abdullah et al. [23] pyrolysed banana pseudo-stem in a bench-scale fluidised bed fast pyrolysis process obtaining 3% gas, 46% bio-oil and 51% bio-char. Feed rate, feeding mode [24], heating rate [25] and response surface optimisation [26] of banana waste pyrolysis have also been studied.

Different types of simulation models to study energy recovery technologies for numerous waste materials readily available in Nigeria have been developed. These include plastics [27], non-edible natural and fossil fuel-based oils [28, 29], glycerol [30], acetic acid [31] and biomass [32–35]. In our previous work on banana pyrolysis [32], a steady-state isothermal (at 500 °C) model for the prediction of pyrolysis product yields based solely on the inherent characteristics of the biomass composition of the different banana wastes was developed. As a sequel to that work, this paper established the temperature relationship for bio-oil production from the different banana wastes via a sensitivity analysis based on a thermodynamic model. Though thermodynamic models have been developed for the pyrolysis of other biomass samples such as rice husk [33, 34] and sugarcane bagasse [35], the approach is currently unreported for banana residues. Besides the aforementioned aim of the paper, plugging this knowledge gap is of keen interest to the authors. A thermodynamic model will give a true understanding of the system behaviour due to temperature effects while eliminating all other extraneous factors. This platform can then help us make a true informed choice on the best residues for each type of product species taking into account their temperature response in the pyrolysis system.

2 Methodology

In this work, the banana (*Musa spp.*) waste pyrolysis process was modelled by the minimisation of Gibbs free energy calculation method on ASPEN Plus V8.8. The method is well discussed in open literature [36, 37]. A cursory review of this method is, however, presented. The equilibrium of a system at constant temperature and pressure can be expressed below in Eq. 1.

$$dG = \sum_{i=1}^K \mu_i n_i dn_i \tag{1}$$

where G is Gibbs free energy, n_i is number of moles of species i , K is total number of chemical species in the reaction mixture and μ_i is chemical potential of species i . The objective is to find the set of n_i values that will result in the smallest G [35]. There are two approaches of doing this:

stoichiometric and non-stoichiometric approach. In the case of the former, the system is described by a system of stoichiometrically independent reactions which are typically chosen arbitrarily from a set of possible reactions. The latter involves finding the equilibrium composition by the direct minimisation of the Gibbs free energy for a given set of species. The non-stoichiometric approach is the more applied technique in open literature [37, 38]. This is because of some advantages such as selection of the possible set of reactions not being required, divergence not occurring during computation and an accurate estimation of the initial equilibrium composition not needed.

$$G = \sum_{i=1}^K \mu_i n_i \tag{2}$$

To find the value of n_i that will give the smallest value of G , we need to ensure that n_i is in mass balance.

$$\sum_{i=1}^K a_{ij} n_i = b_j, \quad j = 1, \dots, M \tag{3}$$

where a_{ij} is number of gram atoms of element j in 1 mol of species i , b_j is total number of gram atoms of element j in the reaction mixture and M is the total number of atomic elements. The above expressions can then be further expressed as Eq. 4

$$G = \sum_{i=1}^K n_i \Delta G_i^0 + RT \sum_{i=1}^K n_i \ln y_i + RT \sum_{i=1}^K n_i \ln P \tag{4}$$

where T is temperature, P is pressure, ΔG_i^0 is standard Gibbs free energy of the formation of species i and y_i is mole fraction of species i . Equation 4 is known as the objective function. Process simulation softwares like ASPEN Plus utilise this in the minimisation of Gibbs free energy calculation method to obtain thermodynamic predictions.

2.1 Simulation specifications

The global stream class was set to 'MIXCINC'. The choice of 'MIXCINC' is made when particle size distribution of the solids is not required and the simulation would only consider conventional components, non-conventional components and solids (without their PSD). Non-conventional components are not present in the ASPEN Plus database. They are specified by their proximate and ultimate analyses. Enthalpy and density are the only properties calculated for non-conventional components from the ultimate and proximate analysis data, and this is done by empirical correlations. The specific property methods for enthalpy and density for banana waste were chosen as HCOALGEN

and DGOALIGT, respectively [32]. Banana (*Musa spp.*) waste is considered as non-conventional material which can be modelled in ASPEN Plus V8.8 in this way. The global calculation method of the simulation was the Peng–Robinson with Boston–Mathias alpha function equation of state (PR-BM). Alpha is a temperature-dependent parameter that improves the pure component vapour pressure correlation at very high temperatures and has been used in pyrolysis simulations on ASPEN Plus [32, 39]. This choice was made because pyrolysis involves high temperatures and the alpha parameter ensures its suitability and higher accuracy when compared to the usual Peng–Robinson EOS.

2.2 Simulation components

The information of the proximate, ultimate and chemical analyses of banana (*Musa spp.*) waste in Table 1 was determined by Kabenge et al. [18]. The proximate analysis presented was, however, re-calculated in a previous paper (with adequate justifications) to make it suitable for ASPEN simulation [32].

Due to the presence of numerous oxygenated organic compounds of different classes in biomass bio-oil, this diversity will need to be properly represented if the simulation is going to give accurate results. A technique used

[40–42] is the selection of a smaller set of compounds with each (or a couple) serving as a representative for a class of organic compound. The criteria for choice are the significance of their proportions in biomass bio-oil. This approach was chosen in this study as opposed to a straight-up choice of aliphatic hydrocarbon as utilised in the previous study [32]. The components added to the simulation were acetic acid, ethylene glycol, acetone, acetaldehyde, formic acid, methanol, formaldehyde, ethanol, phenol and water. Others were propanol, propionic acid, methyl acetate and ethyl formate. The non-conventional biomass feed was broken into simulation components which are the basic biomass constituents: cellulose, hemicellulose and lignin. Hemicellulose and cellulose were represented in the simulation by their monomers: $C_5H_8O_4$ (xylan) and $C_6H_{10}O_5$ (xylose-like cellulose monomer), while lignin was represented by a phenyl propane monomer [32]. The ratios (by mass) of cellulose, hemicellulose and lignin were according to those of experiment presented originally as mass percentages in Table 1. For the synthesis gas, methane, ethane, carbon monoxide and hydrogen gas were added to the simulation.

Biomass ash majorly consists of silicon oxide and it can be as high as 98% [43]. SiO_2 was added to the simulation and considered to represent ash alone. In representing the char in the simulation, certain considerations had to be put in place. Bio-char consists of carbon, hydrogen and other inorganic species in either stacked crystalline graphene sheets or randomly ordered amorphous aromatic structures [20]. The composition of the char and the ratio to which these elements are present vary with pyrolysis temperature [44–46] and from one feedstock to another [16, 46]. The results for only banana leaves bio-char composition [16] at a single temperature were taken as the basis on which char was modelled in the simulation. The weight percentages of ultimate analysis by Sellin et al. [16] for banana leaves bio-char were converted to molar percentages (by dividing by the molar mass of each atom species). These molar percentages were then normalised to give the formulae $C_{1.0}H_{0.8}O_{0.7375}N_{0.0215}S_{0.0025}$. This compound as well as carbon graphite were added to the simulation as solids. Sulphur in the biomass was present only in the case of the pseudo-stem, and it was considered to remain in the char (as organic sulphur). The nitrogen content of the biomass was accounted by the addition of pyrrole [32, 41] which formed a part of the liquid phase (though some of the nitrogen was present in the char too).

2.3 Pyrolysis model description

The pyrolyser was modelled in the simulation by three stages. Each stage was used to represent certain aspects of the pyrolysis process. A combination of RYIELD and RGIBBS

Table 1 Proximate and ultimate analysis of different banana (*Musa spp.*) wastes [18, 32]

	Pseudo-stem	Peel	Leaves
Proximate analysis (wt% dry basis)			
Moisture	7.98	11.56	6.67
Fixed carbon	1.12	2.39	7.09
Volatile matter	82.29	77.84	77.79
Ash	8.61	8.21	8.45
Ultimate/elemental analysis (wt% dry basis)			
Carbon	33.46	35.65	38.57
Hydrogen	6.44	6.19	6.44
Sulphur	0.04	NL	NL
Oxygen	49.94	45.94	43.49
Nitrogen	0.8	1.94	0.8
Ash	9.36	9.28	9.05
Chemical analysis (wt%)			
Cellulose	38.48	9.9	35.58
Hemicelluloses	25.36	41.38	23.46
Lignin	5.77	8.9	10.58
Extractives	NS	NS	NS
Heating/calorific values (MJ/Kg)			
High heating value	15.04	16.15	17.57
Low heating value	13.63	14.80	16.16

NS Not stated, NL negligible

blocks was implemented. The RYIELD block converts the non-conventional feedstock to conventional simulation components (cellulose, hemicellulose and lignin). The RYIELD and RGIBBS blocks do not require the specification reaction stoichiometry. The calculator block is used to specify some conversion rules to which the RYIELD has to obey in the form of executable FORTRAN statements. The fixed carbon from the proximate analysis is equated to a carbon mass yield. Moisture is equated to a water mass yield and volatile matter is equated to the summation of cellulose, hemicellulose and lignin, while ash is equated to silicon oxide solid. The volatiles are equated to the three basic components based on mass fractions calculated from the chemical analysis presented in Table 1. An equal set of mass flows of the output species was specified at the RYIELD block, but the block scales up the output flowrate to ensure mass balance, while the calculator block imposes the FORTRAN statements representing the conversion rules. The RGIBBS block does the calculation of chemical and phase equilibrium through the minimisation of Gibbs free energy. This is the actual thermodynamic prediction of the pyrolysis process. The first RGIBBS block does the calculations of chemical equilibrium only, while the second RGIBBS block does the calculations of phase equilibrium only. The RGIBBS block in ASPEN Plus cannot do phase and chemical equilibrium calculations simultaneously for a multiphase stream. Hence, the first Gibbs block was set to 'calculate both chemical and phase equilibrium' (though will only compute for chemical equilibrium because it is a multiphase stream), and the second Gibbs block was set to 'calculate phase equilibrium'.

2.4 Process summary

The thermodynamic model implemented on the ASPEN Plus flowsheet is sequential modular. The idea of sequencing generally connotes designating the order of performance of tasks to assure optimal utilisation of available inputs [47]. Hence, a sequential block-by-block calculation method where the results of one module serve as the basis for the next is done by the software. The simulation ambient temperature and pressure were specified as 25 °C and 1 atm, respectively. The banana (*Musa spp.*) waste (100 kg/h) was fed into the system at ambient conditions without the consideration of particle sizes. The process flow diagram (PFD) of the simulation is presented in Fig. 1.

The RYIELD block carried out the conversion of the non-conventional components. The split fractions were specified by the calculator block, using the values in the chemical analysis earlier stated. The temperature and pressure of the reactor system are taken as the temperature and pressure of both RGIBBS block, and they are set at similar temperature and pressure conditions at all times. The cyclone is used to model the separation of the char from the vapour products. The vapours are then condensed to ambient conditions before the final separation of the non-condensable gas from the oil.

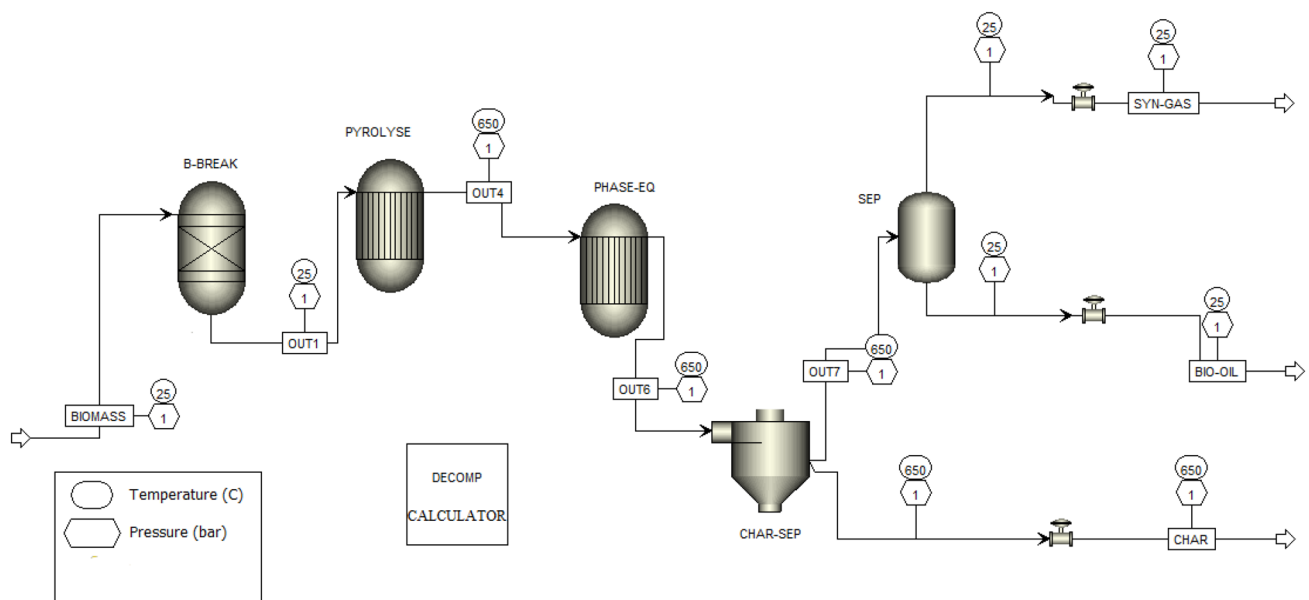


Fig. 1 Process flow diagram of the pyrolysis simulation

3 Results and discussion

Upon implementation of the methodology elucidated in the previous section, the simulation was run successfully without errors. The key model parameters that determine the results obtained from the model are the ultimate and proximate analyses information, the cellulose–hemicellulose–lignin ratio and the process temperature. The model predictions are examined and validated in the next subsection in the light of other experimental results.

3.1 Validation of thermodynamic model

The results of the sensitivity analysis of the fast pyrolysis of banana pseudo-stem conducted by Abdullah et al. [23] were used to validate this study. Of the studies reporting the pyrolysis of banana wastes [22–26], theirs alone gave a report of temperature sensitivity. Some discrepancies with fast pyrolysis results will be present due to differences in the systems. The thermodynamic predictions are essentially results at chemical and phase equilibrium. In most cases, product elutriation in fast pyrolysis system (especially those of semi-batch and continuous mode) occurs in the absence of chemical equilibrium as the composition profile of the product stream is still changing. Abdullah et al. [23] utilised a bench-scale fluidised bed reactor (continuous mode) in their work with residence time of only a few seconds. In summary, model results will not always perfectly align with every reported experiments because the results of the former are at chemical and phase equilibrium which is not always the case for pyrolysis systems especially those with very high heating rate and short residence time.

Figure 2 reveals the temperature sensitivity of gas yield in comparison with experiments. The model accurately shows the relationship between temperature and gas yield albeit being an over-prediction. Experiments also reveal a steeper climb in the gas yield than model predictions. Gas yield at thermodynamic equilibrium will always tend to be higher than fast pyrolysis results as the maximum possible cracking of the large molecular weight chemical species in the system at that temperature would have been achieved. Furthermore, other similar thermodynamic studies have revealed that the higher temperatures lead to higher intensity of cracking of the chemical species present. This leads to an increase in the presence of low molecular weight compounds which would most likely exist in the vapour phase at ambient conditions [33] hence a higher gas yield.

From Fig. 3, we observe that the trend of oil yield with temperature is only captured by the model above 550 °C.

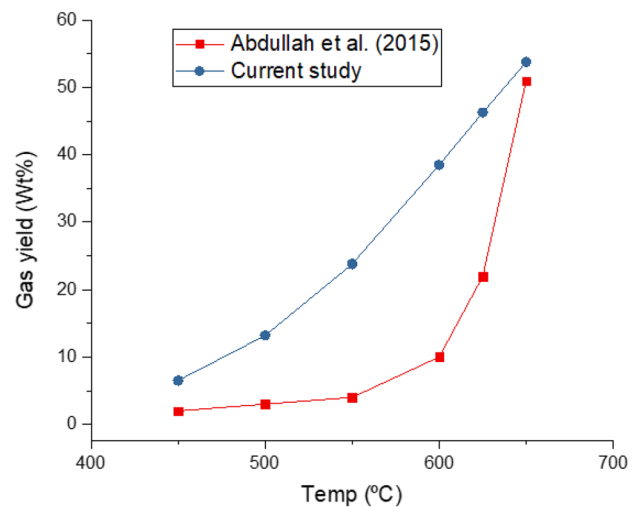


Fig. 2 Banana pseudo-stem pyrolysis gas yield

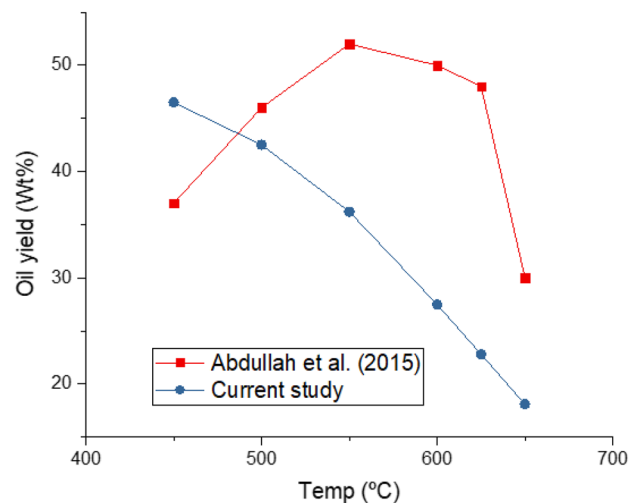


Fig. 3 Banana pseudo-stem pyrolysis oil yield

Below this temperature, experiments show a fall in oil yield with temperature. The experiment by Abdullah et al. [23] is a fast pyrolysis process, one at which chemical equilibrium in the fluid phase is usually not achieved before product elutriation. They used a residence time of 3 s in their study. Tsai et al. [48] explained that the initial rise in oil yield with temperature (for fast pyrolysis) is due to the absence of secondary reactions. Thus, the maxima of 550 °C were not captured by the thermodynamic predictions. The current model is also generally an under-prediction of experiments. This can also be attributed to the earlier stated reason of thermodynamic equilibrium in the simulation model. Overall, the fall in oil yield at elevated temperatures is due to the breakdown of the

oil-phase compounds into gaseous products occurring due to secondary reactions [33].

From Fig. 4, it can be observed that the model excellently captures the relationship between char yield and process temperature. However, the model under-predicts at temperatures below 625 °C and vice versa. The decrease in char at higher temperatures is due to the greater primary decomposition and cracking of the chemical species in the pyrolysis system, leading to a greater proportion of compounds that would exist in the fluid phase at ambient conditions [49]. The yield of char drops with increasing temperature as there is a higher intensity of cracking of the chemical species. This is always the case in most pyrolysis experiments involving various feedstock. It can be summarised that the model is a good fit and predictor of pyrolysis products especially for char and gas yield.

Statistical analysis of the data was done using SPSS v17.0 and is shown in Tables 2. The model values were compared with the validation literature data to determine the accuracy of the thermodynamic model. The two key indices are the correlation and the statistical significance (*p* value). In Table 2, the value of *N* as 6 indicates that there are 6 data points for each of the data series on pairs 1–3. This can also be seen as there are 6 sets of data points on the plots in Figs. 2, 3 and 4, respectively. It can be observed that the model predictions for gas yield (pair 1), oil yield (pair 2) and char yield (pair 3) all show a positive correlation with the literature. However, only gas and char results show strong positive correlation (values close to 1.0). The gas and char yield are statistically significant (at *p* < 0.05), but oil values are not. This is expected as the model was only able to capture the literature trend for oil at temperatures above 550 °C. Having established the extent of accuracy of the model, we can proceed to compare the

Table 2 Paired samples correlations

Pairs	<i>N</i>	Correlation	Sig.
Pair 1 Gas_Literature and Gas_Model	6	0.840	0.036
Pair 2 Oil_Literature and Oil_Model	6	0.175	0.741
Pair 3 Char_Literature and Char_Model	6	0.971	0.001

different banana wastes and try and understand what potentials they hold for biofuels production.

3.2 Temperature sensitivity and comparison

In this section, the product yields of the different banana wastes are compared. A comparative study is valid because the same model will be applied in each case. The differences will be the input of the proximate, ultimate and chemical analysis. These will form the basis of the interpretations of the results obtained.

From Fig. 5, it can be observed that the thermodynamic predictions of gas yield are similar for the different feedstock at low temperatures but vary at higher temperatures with the leaves seemingly producing less gas than the other banana wastes considered. The pseudo-stem was observed to give a slightly higher yield of gas compared to the other residues. Results by Fernandes et al. [17] for slow pyrolysis showed that at 850 °C pseudo-stem gas yield was higher than for leaves. In general, the increase in gas yield with temperature is due to the greater intensity of cracking of the chemical species in the system, thereby leading to more vapour phase products [33].

From Fig. 6, it is noticed that the yield of oil from leaves is less than that for pseudo-stem and peels. From the proximate analysis information in Table 1, it is seen

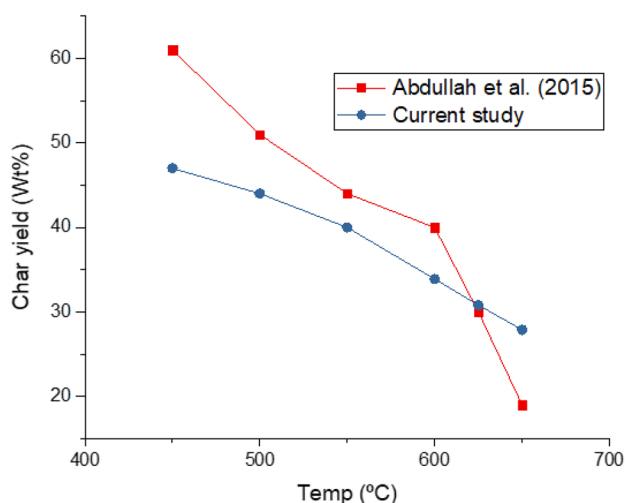


Fig. 4 Banana pseudo-stem pyrolysis char yield

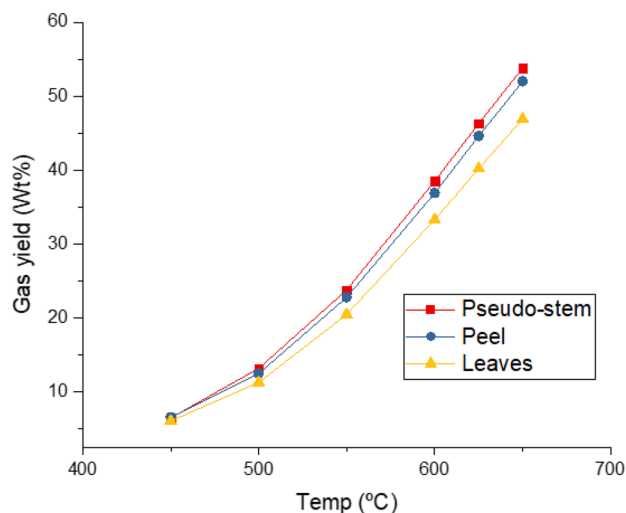


Fig. 5 Gas yield of banana waste pyrolysis

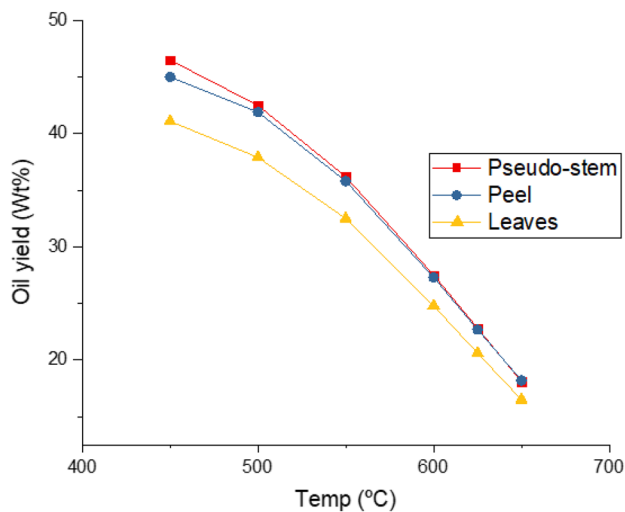


Fig. 6 Oil yield of banana waste pyrolysis

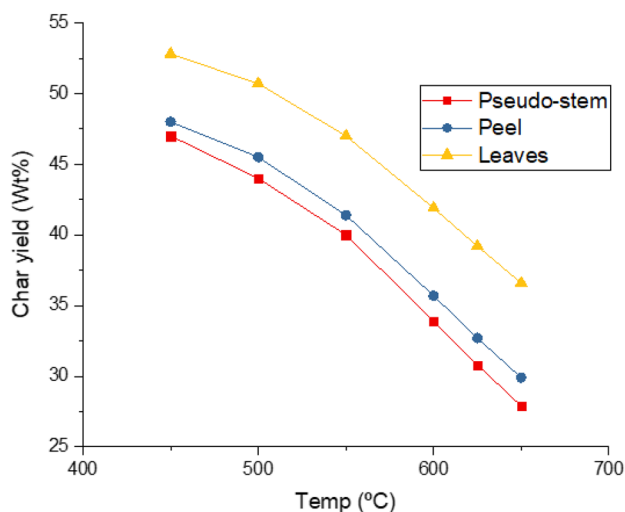


Fig. 7 Char yield of banana waste pyrolysis

that the amount of volatile matter in leaves is significantly lesser than for pseudo-stem. This of course can be a key reason for the lesser yield for leaves. Though the volatile matter content of the leaves is similar to that of peels, certain markers justify the lesser oil yield of the leaves. A lesser proportion of oxygen (from the ultimate analysis) in the leaves compared to the peels means lesser oxygenated organic compounds in the products. These oxygenated organic compounds make up the bulk of the liquid phase. In general, it can be surmised that the fluid phase products (bio-oil and syn-gas) are higher for pseudo-stem than for the other residues. This is in agreement with the proximate analysis result in Table 1 where the volatile matter content of the pseudo-stem is higher than for the other residues.

Figure 7 reveals a higher char yield for leaves than for the other banana residues. The carbon content of the leaves (from the ultimate analysis in Table 1) is higher than for the other residues, while the oxygen is the lowest. These are pointers towards a high char-yielding feedstock. This is also supported by the results of the proximate analysis where the leaves possess a significantly higher proportion of fixed carbon than the other residues. In general, the decrease in char at higher temperatures is due to the greater primary decomposition and cracking of the chemical species in the pyrolysis system, leading to a greater proportion of compounds that would exist in the fluid phase at ambient conditions [49].

4 Conclusion

The model validation revealed that the thermodynamic model accurately shows the relationship between temperature and pyrolysis product yield (especially for gas and char). Having established the suitability of the model, a comparison of the different feedstock for biofuels production was carried and justifications were given for results obtained. Thermodynamic predictions of gas yield were similar for the different feedstock at low temperatures but vary at higher temperatures with the leaves producing less. The pseudo-stem was observed to give a slightly higher yield of gas compared to the other residues. It was also established that the yield of oil from leaves is less and that of char is higher than for pseudo-stem and peels. It was surmised that the fluid phase products (bio-oil and syn-gas) are higher for pseudo-stem than for the other residues. This is in agreement with the proximate analysis result where the volatile matter content of the pseudo-stem was higher than for the other residues. A key conclusion from this paper is the suitability of banana pseudo-stem for bio-oil production compared to the other residues studied. The leaves and peel will be more suitable for low-temperature thermochemical processing for bio-char production like those discussed by Adeniyi et al. [50] and Adeniyi et al. [51].

Acknowledgements The authors would love to duly acknowledge the input of the process simulation unit of the Department of Chemical Engineering, University of Ilorin, Nigeria. No official funding or grant was received for this research.

Compliance with ethical standards

Conflict of interest The authors declare that they have no conflict of interest.

References

- Abdullah N, Sulaiman F, Taib RM (2013) Characterization of banana (*Musa* spp.) plantation wastes as a potential renewable energy source. In: AIP conference proceedings. AIP, vol 1, pp 325–330. <http://dx.doi.org/10.1063/1.4803618>
- Tock JY, Lai CL, Lee KT, Tan KT, Bhatia S (2010) Banana biomass as potential renewable energy resource: a Malaysian case study. *Renew Sustain Energy Rev* 14(2):798–805. <https://doi.org/10.1016/j.rser.2009.10.010>
- Abdullah N, Sulaiman F, Miskam MA, Taib RM (2014) Characterization of banana (*Musa* spp.) pseudo-stem and fruit-bunch-stem as a potential renewable energy resource. *Int J Biol Vet Agric Food Eng* 8(8):712
- Maneerat N, Tangsuphoom N, Nitithamyong A (2017) Effect of extraction condition on properties of pectin from banana peels and its function as fat replacer in salad cream. *J Food Sci Technol* 54(2):386–397. <https://doi.org/10.1007/s13197-016-2475-6>
- Oliveira TÍS, Rosa MF, Cavalcante FL, Pereira PHF, Moates GK, Wellner N, Mazzetto SE, Waldron KW, Azeredo HM (2016) Optimization of pectin extraction from banana peels with citric acid by using response surface methodology. *Food Chem* 198:113–118. <https://doi.org/10.1016/j.foodchem.2015.08.080>
- Adeniyi AG, Ighalo JO, Onifade DV (2019) Banana and plantain fiber reinforced polymer composites. *J Polym Eng* 39(7):597–611. <https://doi.org/10.1515/polypeng-2019-0085>
- Mahaboob S (2011) Banana fiber reinforced composite materials. IIT Ropar. <https://www.slideshare.net/SajeedMahaboob/banana-fiber-reinforced-composite-materials>. Accessed 3 July 2019
- Sustainable Textile Innovations: Banana Fibres (2017) <https://www.google.com/amp/s/fashionunited.uk/news/fashion/sustainable-textile-innovations-banana-fibre/2017082825623/amp>. Accessed 2 July 2019
- Ince M, Ince OK, Yonten V, Karaşlan NM (2016) Nickel, lead, and cadmium removal using a low-cost adsorbent-banana peel. *At Spectrosc* 37(3):125–130
- El-Gendy AA, Mohamed SH, Abd-Elkader AH (2013) Ion exchanger from chemically modified banana leaves. *Carbohydr Polym* 96(2):481–486. <https://doi.org/10.1016/j.carbpol.2013.04.031>
- Rana GK, Singh Y, Mishra S, Rahangdale HK (2018) Potential use of banana and its by-products: a review. *Int J Curr Microbiol Appl Sci* 7(6):1827–1832. <https://doi.org/10.20546/ijcma.s.2018.706.218>
- Mohapatra D, Mishra S, Sutar N (2010) Banana and its by-product utilisation: an overview. *J Sci Ind Res* 69:323–329
- Sugumaran P, Susan VP, Ravichandran P, Seshadri S (2012) Production and characterization of activated carbon from banana empty fruit bunch and *Delonix regia* fruit pod. *J Sustain Energy Environ* 3(3):125–132
- Bilba K, Arsene M-A, Ouensanga A (2007) Study of banana and coconut fibers: botanical composition, thermal degradation and textural observations. *Biores Technol* 98(1):58–68. <https://doi.org/10.1016/j.biortech.2005.11.030>
- Vargas Solis DC, Gorugantu SB, Carstensen H-H, Streitwieser DA, Van Geem K, Marin G (2017) Product distributions from fast pyrolysis of 10 Ecuadorian agricultural residual biomass samples. In: 10th international conference on chemical kinetics (ICCK)
- Sellin N, Krohl DR, Marangoni C, Souza O (2016) Oxidative fast pyrolysis of banana leaves in fluidized bed reactor. *Renew Energy* 96:56–64. <https://doi.org/10.1016/j.renene.2016.04.032>
- Fernandes E, Marangoni C, Medeiros S, Souza O, Sellin N (2012) Slow pyrolysis of banana culture waste: leaves and pseudostem. In: 3rd international conference on industrial and hazardous waste management
- Kabenge I, Omulo G, Banadda N, Seay J, Zziwa A, Kiggundu N (2018) Characterization of banana peels wastes as potential slow pyrolysis feedstock. *J Sustain Dev* 11(2):14. <https://doi.org/10.5539/jsd.v11n2p14>
- Pereira AL, do Nascimento DM, Cordeiro EM, Morais JP, Souza Filho M, Rosa MDF (2010) Characterization of lignocellulosic materials extracted from the banana pseudostem. In: 7th international symposium on natural polymers and composites, proceedings, Embrapa Agroindústria Tropical-Artigo em anais de congresso (ALICE), Gramado, Brazil. Associação Brasileira de Polímeros, São Carlos
- Jahirul MI, Rasul MG, Chowdhury AA, Ashwath N (2012) Biofuels production through biomass pyrolysis—a technological review. *Energies* 5(12):4952–5001. <https://doi.org/10.3390/en5124952>
- Navarro-Mtz A, Urzua-Valenzuela M, Morelos-Pedro M (2017) Hydrogen production from non-conventional biomass pyrolysis. *Inorg Chem Indian J* 12(1):107
- Manocha S, Bhagat JH, Manocha LM (2001) Studies on pyrolysis behaviour of banana stem as precursor for porous carbons. *Carbon Lett* 2(2):91–98
- Abdullah N, Sulaiman F, Taib RM, Miskam MA (2015) Pyrolytic oil of banana (*Musa* spp.) pseudo-stem via fast process. In: AIP conference proceedings. AIP Publishing, vol 1, p 100005. <http://dx.doi.org/10.1063/1.4915212>
- Abdullah N, Sulaiman F, Taib RM (2013) Feeding of banana (*Musa* spp.) plantation wastes for fast pyrolysis process. In: AIP conference proceedings, 2013. AIP, vol 1, pp 346–350. <http://dx.doi.org/10.1063/1.4803622>
- Cheng Q, Jiang M, Chen Z, Wang X, Xiao B (2016) Pyrolysis and kinetic behavior of banana stem using thermogravimetric analysis. *Energy Sources Part A Recov Util Environ Eff* 38(22):3383–3390. <https://doi.org/10.1080/15567036.2016.1153754>
- Omulo G, Banadda N, Kabenge I, Seay J (2019) Optimizing slow pyrolysis of banana peels wastes using response surface methodology. *Environ Eng Res* 24(2):354–361. <https://doi.org/10.4491/eer.2018.269>
- Adeniyi AG, Eletta AAO, Ighalo JO (2018) Computer aided modelling of low density polyethylene pyrolysis to produce synthetic fuels. *Nig J Technol* 37(4):945–949. <https://doi.org/10.4314/njt.v37i4.12>
- Adeniyi AG, Ighalo JO, Eletta AAO (2018) Process integration and feedstock optimisation of a two-step biodiesel production process from *Jatropha Curcas* using aspen plus. *Chem Prod Process Model*. <https://doi.org/10.1515/cppm-2018-0055>
- Adeniyi AG, Adewoye LT, Ighalo JO (2018) Computer aided simulation of the pyrolysis of waste lubricating oil using aspen hysys. *J Environ Res Eng Manag* 74(2):52–57. <https://doi.org/10.5755/j01.erem.74.2.20537>
- Adeniyi AG, Ighalo JO (2018) Study of process factor effects and interactions in synthesis gas production via a simulated model for glycerol steam reforming. *Chem Prod Process Model*. <https://doi.org/10.1515/cppm-2018-0034>
- Adeniyi AG, Ighalo JO, Otoikhian KS (2019) Steam reforming of acetic acid: response surface modelling and study of factor interactions. *Chem Prod Process Model*. <https://doi.org/10.1515/cppm-2019-0066>
- Adeniyi AG, Ighalo JO, Amosa KM (2019) Modelling and simulation of banana (*Musa* spp.) waste pyrolysis for bio-oil production. *Biofuels*. <https://doi.org/10.1080/17597269.2018.1554949>
- Adeniyi AG, Odetoye TE, Titiloye J, Ighalo JO (2019) A thermodynamic study of rice husk (*Oryza Sativa*) pyrolysis. *Eur J Sustain Dev Res*. <https://doi.org/10.29333/ejosdr/5830>
- Adeniyi AG, Ighalo JO, Aderibigbe FA (2019) Modelling of integrated processes for the pyrolysis and steam reforming of rice

- husk (*Oryza sativa*). SN Appl Sci. <https://doi.org/10.1007/s42452-019-0877-6>
35. Adeniyi AG, Ighalo JO, Abdulsalam A (2019) Modelling of integrated processes for the recovery of the energetic content of sugarcane bagasse. *Biofuels Bioprod Biorefin*. <https://doi.org/10.1002/bbb.1998>
 36. Adeniyi AG, Otoikhian KS, Ighalo JO (2019) Steam reforming of biomass pyrolysis oil: a review. *Int J Chem Reactor Eng*. <https://doi.org/10.1515/ijcre-2018-0328>
 37. Adeniyi AG, Ighalo JO (2019) A review of steam reforming of glycerol. *Chem Pap*. <https://doi.org/10.1007/s11696-019-00840-8>
 38. Adeniyi AG, Otoikhian KS, Ighalo JO (2019) Steam reforming of biomass pyrolysis oil: a review. *Int J Chem React Eng*. <https://doi.org/10.1515/ijcre-2018-0328>
 39. Altayeb RK (2015) Liquid fuel production from pyrolysis of waste tires: process simulation, exergetic analysis, and life cycle assessment. Masters thesis, American University of Sharjah, Sharjah, United Arab Emirates
 40. Ward J, Rasul MG, Bhuiya MMK (2014) Energy recovery from biomass by fast pyrolysis. *Procedia Eng* 90(90):669–674. <https://doi.org/10.1016/j.proeng.2014.11.791>
 41. Peters JF, Iribarren D, Dufour J (2013) Predictive pyrolysis process modelling in Aspen Plus. In: 21st European biomass conference and exhibition
 42. Iordanidis A, Kechagiopoulos P, Voutetakis S, Lemonidou A, Vasalos I (2006) Autothermal sorption-enhanced steam reforming of bio-oil/biogas mixture and energy generation by fuel cells: concept analysis and process simulation. *Int J Hydrogen Energy* 31(8):1058–1065. <https://doi.org/10.1016/j.ijhydene.2005.10.003>
 43. Alvarez J, Lopez G, Amutio M, Bilbao J, Olazar M (2014) Bio-oil production from rice husk fast pyrolysis in a conical spouted bed reactor. *Fuel* 128:162–169. <https://doi.org/10.1016/j.fuel.2014.02.074>
 44. Fu P, Hu S, Xiang J, Sun L, Li P, Zhang J, Zheng C (2009) Pyrolysis of maize stalk on the characterization of chars formed under different devolatilization conditions. *Energy Fuels* 23(9):4605–4611. <https://doi.org/10.1021/ef900268y>
 45. Kim KH, Kim J-Y, Cho T-S, Choi JW (2012) Influence of pyrolysis temperature on physicochemical properties of biochar obtained from the fast pyrolysis of pitch pine (*Pinus rigida*). *Biores Technol* 118:158–162. <https://doi.org/10.1016/j.biortech.2012.04.094>
 46. Chen Y, Zhang X, Chen W, Yang H, Chen H (2017) The structure evolution of biochar from biomass pyrolysis and its correlation with gas pollutant adsorption performance. *Biores Technol* 246:101–109. <https://doi.org/10.1016/j.biortech.2017.08.138>
 47. Licker DM (2003) Dictionary of engineering, 2nd edn. Mc-Graw Hill Publishers, Chicago
 48. Tsai W, Lee M, Chang Y (2007) Fast pyrolysis of rice husk: product yields and compositions. *Biores Technol* 98(1):22–28. <https://doi.org/10.1016/j.biortech.2005.12.005>
 49. Natarajan E, Ganapathy SE (2009) Pyrolysis of rice husk in a fixed bed reactor. *World Acad Sci Eng Technol* 56:504–508
 50. Adeniyi AG, Ighalo JO, Onifade DV (2019) Production of biochar from plantain (*Musa paradisiaca*) fibers using an updraft biomass gasifier with retort heating. *Combust Sci Technol*. <https://doi.org/10.1080/00102202.2019.1650269>
 51. Adeniyi AG, Ighalo JO, Onifade DV (2019) Production of biochar from elephant grass (*Pennisetum purpureum*) using an updraft biomass gasifier with retort heating. *Biofuels*. <https://doi.org/10.1080/17597269.2019.1613751>

Publisher's Note Springer Nature remains neutral with regard to jurisdictional claims in published maps and institutional affiliations.